Available online at www.sciencedirect.com
SCIENCE DIRECT®
Journal of the European Ceramic Society 25 (2005) 1531–1540
www.elsevier.com/locate/jeurceramsoc

Sintering behaviour of a glass obtained from MSWI ash

Alexander Karamanov*, Mirko Aloisi, Mario Pelino

Department of Chemistry, Chemical Engineering and Materials, University of L'Aquila, 67040 Monteluco di Roio, L'Aquila, Italy

Received 5 March 2004; received in revised form 19 May 2004; accepted 31 May 2004
Available online 15 September 2004

Abstract

The sintering behaviour of a glass obtained by Municipal Solid Waste Incinerator (MSWI) bottom ash (WG) was investigated and compared with a Na_2O–MgO–CaO–SiO_2 composition (CG). The sintering activation energy, E_{sin}, and the energy of viscous flow, E_η, were evaluated by dilatomeric measurements at different heating rates. The formation of crystalline phases was evaluated by Differential Thermal Analysis (DTA) and X-Ray Diffraction (XRD), and observed by Scanning Electron Microscopy (SEM) and Transition Electron Microscopy (TEM). In CG, the sintering started at $\approx 10^{13}$ dPa s viscosity and E_{sin} (245 kJ/mol) remains constant in the measured range of shrinkage, up to 9%. In WG the densification started at $\approx 10^{11}$ dPa s, E_{sin} resulted to be 395 kJ/mol up to 5% shrinkage, 420 kJ/mol at 8% and 485 kJ/mol at 10% shrinkage. The sintering rate decreased due to the beginning of the pyroxene formation and the densification stopped in the temperature range 1073–1123 K after formation of 5 ± 3% and 13 ± 3% crystal phase, at 5 and 20 K/min, respectively. Higher densification and improved mechanical properties were obtained by applying the fast heating rate, i.e. 20 K/min.

Keywords: Glass-ceramics; Sinter-crystallization; Industrial wastes; Waste materials

1. Introduction

The development of the sintering theory started in the middle of the twentieth century by the work of Frenkel[1] and, as noted by several authors,[2–4] made significant progress in the past 25 years. In some experiments, nevertheless, the existing theories are not able to exhaustively describe the complex aspects arising during the sintering process. An example is the sinter-crystallization, applied to produce sintered glass-ceramics,[5] where the densification and the phase formation take place in the same temperature interval.

Since the crystallization starts on the surface, many authors assume that the sintering rate is a function of the grain area, free of crystal;[6–8] it is expected that the densification process stops when the grain surface is all covered by crystals. This elegant model, however, does not examine the influence of the liquid–liquid separation, bulk nucleation and/or crystal growth on the sintering.

The densification tendency is considerably lower when bulk crystallization takes place,[9] due to the increasing of the apparent viscosity in the bulk of the particles during the phase formation.[10–15] The apparent viscosity may increase significantly by liquid-liquid separation, nucleation or/and crystal growth phenomena,[5,16] reaching values 10^4–10^6 times higher than the shear viscosity of the parent melts. An example is the glass-ceramics production cycle, where the rise of the heating rate between the nucleation and crystallization steps depends on the increasing of the apparent viscosity: at low heating rate, due to the formation of a crystal phase, the apparent viscosity increases thus avoiding the deformation of the products; at a high heating rate the glass-ceramic may be deformed under its own weight.[5,16]

When a crystallization trend is too high, the sintering rate may be considerably reduced, leading to residual porosity and decreasing of the mechanical properties. This behaviour was observed in several glass compositions obtained by melting industrial wastes; typical examples are the glasses, obtained from Municipal Solid Waste Incinerator (MSWI) ashes.[17–20]

* Corresponding author. Tel.: +39 0862 434233; fax: +39 0862 434233.
E-mail address: karama@ing.univaq.it (A. Karamanov).

0955-2219/$ – see front matter © 2004 Elsevier Ltd. All rights reserved.
doi:10.1016/j.jeurceramsoc.2004.05.023

The kinetics of sintering of a glass obtained by melting MSWI bottom ashes is presented in this work. The sintering rate and the sintering activation energy, E_{sin}, were evaluated by dilatometric measurements at various heating rates. The dilatometric technique was also applied to estimate the energy of viscous flow, E_η, in the glass-transition region. The formation of crystalline phases in the glass, during sintering, was evaluated by Differential Thermal Analysis (DTA), X-Ray Diffraction (XRD), Transmission Electron Microscopy (TEM) and Scanning Electron Microscopy (SEM).

2. Mathematical approaches

The densification is related to bulk transport (grain-boundary diffusion, volume diffusion or viscous flow) or surface transport (surface diffusion or evaporation-condensation) mechanisms. In the case of bulk transport, the sintering is accompanied by a linear shrinkage of the body, which is related to the variables by the following equation:[21]

$$\frac{d(\Delta L/L_0)}{dt} = A_0 T^a \exp\left(\frac{-E_{sin}}{RT}\right)\left(\frac{\Delta L}{L_0}\right)^{1-n/2} \quad (1)$$

where $(\Delta L/L_0)$ is the linear shrinkage, t is the time, A_0T^a is an Arrhenius pre-exponential factor at a constant particles size, T is the temperature, E_{sin} is the activation energy of the sintering, a and n are constant depending on the transport mechanism. In the case of sintering by viscous flow $n = 2$ and $a = 0$ and Eq. (1) may be rewritten in the following simplest form:

$$\frac{d(\Delta L/L_0)}{dt} = A_0 \exp\left(\frac{-E_{sin}}{RT}\right) \quad (2)$$

Similar equations may also be obtained through the classical Frenkel equation:[1]

$$\frac{d(\Delta L/L_0)}{dt} = \frac{3\sigma}{8r\eta(T)} \quad (3)$$

where σ is the surface tension, η is the viscosity and r is the particle radius. These relations may be applied for the initial stage of neck growth, i.e. in the 0–10% range of linear shrinkage.[2,8]

The activation energy of viscous flow, E_η, for a glass forming composition, decreases with the increasing of the temperature.[22,23] However, for a relatively short temperature interval, E_η may be considered as a constant and evaluated by an Arrhenius equation, so that Eq. (3) becomes similar to Eq. (2) being E_{sin} equivalent to E_η.

In non-isothermal conditions at a constant heating rate, v, Eq. (2) becomes:

$$\frac{d(\Delta L/L_0)}{dT} = \frac{A_0}{v} \exp\left(\frac{-E_{sin}}{RT}\right) \quad (4)$$

After integration,[24,25] Eq. (4) gives the following expression:

$$\ln\left(\frac{v}{T_X^2}\right) = \frac{-E_{sin}}{RT_X} \quad (5)$$

where T_X is the temperature at which the sintering process attains a fixed shrinkage value X. Eq. (5) can be applied to evaluate the values of E_{sin} using dilatometric results, obtained at different heating rates.

Similar equations are widely used for other transformation processes, such as crystallization[26] (equations of Kissinger,[27] Thakur[28] and Ozawa[29]) or glass transition (equations of Bartenev[23] and Chen[25]).

3. Experimental

A glass, labelled WG, was obtained by melting 500 g of MSWI bottom ashes in a corundum crucible at 1673 K. After 1 h holding, the melt was quenched on a steel mould. Part of the glass was broken and milled, while another was annealed, cut and polished into 4 mm × 4 mm × 25 mm samples. A second glass, labelled CG, was prepared in the oxides Na_2O–MgO–CaO–SiO_2 system with a composition free of crystallization phenomena in the investigated temperature range. The chemical analyses of the two glasses, obtained by a Spectro-Xepos X-ray fluorescence apparatus, are reported in Table 1.

The "green" samples with 10 mm × 4 mm × 4 mm size of WG and CG were prepared by mixing the 45–75 μm powder fractions with a 7% PVA solution and by pressing at 100 MPa. After drying and a preliminary 30 min step at 553 K (to eliminate the PVA) the samples were treated in "Netzsch 402 ED" differential dilatometer at 5, 10 and 20 K/min heating rates in the 600–1300 K temperature interval. By using the 4 mm × 4 mm × 25 mm monolithic samples, the glass transformation temperatures, T_g, and dilatometric softening points, T_s, were

Table 1
Chemical compositions of the investigated compositions (wt.%)

	WG	CG
SiO_2	46.14	72.02
TiO_2	1.12	0.05
Al_2O_3	14.07	0.17
Cr_2O_3	0.12	0.01
Fe_2O_3	6.42	0.18
CaO	14.73	10.08
MgO	3.53	2.79
BaO	0.23	0.05
ZnO	0.32	–
PbO	0.11	–
CuO	0.19	–
NiO	0.02	–
MnO	0.16	0.01
Na_2O	10.32	13.94
K_2O	1.16	0.68

obtained, for the WG and CG glasses, at 3, 5 and 10 K/min heating rates.

The crystallization of WG in non-isothermal conditions was evaluated by DTA, using about 100 mg of powder samples (45–75 μm). The crystalline phases formed during the heat-treatments were determined by XRD technique (Philips PW1830 apparatus and Cu Kα radiation). The percentages of crystal phase formed were measured by comparing the intensity of the amorphous halo in the parent glass and the heat-treated samples, respectively.[16]

The morphology of the heat-treated at different temperatures samples was examined by Scanning Electron Microscopy (Philips XL30CP) on fractured specimen surface and by Transmission Electron Microscopy (Philips 200 keV) using fine powders (<10 μm).

In order to evaluate the mechanical properties, two series of five samples (50 mm × 4 mm × 3 mm) were sintered for 1 h at 1173 K at 5 and 20 °C/min heating rates, respectively. The Young modulus was determined by means of the non-destructive resonance frequency technique (Grindosonic) and then the bending strength was evaluated by a three point bending test with 40 mm outer span and a speed of 0.1 mm/min (SINTEC D/10).

4. Results and discussion

The sintering dilatometric curves and their derivates (i.e. the variation of the sintering rate as function of the temperature) of WG and CG at 5, 10 and 20 K/min are plotted in Figs. 1 and 2, respectively.

In CG composition, due to the decreasing of the viscosity by increasing the temperature, a sample deformation occurred in the dilatometer holder after 9–10% shrinkage, therefore the sintering experiments were stopped at this shrinkage value. In agreement with the decreasing of the viscosity, continuous increasing of the sintering rate with the rise of the temperature was measured.

In WG, no deformation was observed and the shrinkage of the samples stopped after 10–14% depending on the heating rate. Figs. 1 and 2 show that the sintering rates increase up to 4–5% shrinkage and decrease after 7–8%. The higher sintering rate occurs at 1060 K for 5 K/min, 1075 K for 10 K/min and 1095 K for 20 K/min, corresponding to a shrinkage values of about 6, 7 and 8%, respectively.

These results were confirmed by the evaluation of the sintering activation energy, E_{sin}, of CG and WG, obtained by Eq. (5) and plotted, as function of the shrinkage, in Fig. 3. The activation energy of CG is 245 ± 10 kJ/mol in the whole investigated range, while the E_{sin} plot for WG shows a variation of the trend, i.e. E_{sin} increases after 6% shrinkage, being 395 ± 10 kJ/mol at 5%, 420 ± 10 kJ/mol at 8% and 485 ± 15 kJ/mol at 10% shrinkage, respectively.

The E_{sin} values were compared with the corresponding activation energies of the viscous flow, E_η, obtained by a relationship similar to Eq. (5).[25] Fig. 4 shows the dilatometric curves at different heating rates. Fig. 5 depicts the plots of $\ln(v/T_g^2)$ versus $1/T_g$ and the corresponding values of the E_η. The T_g range and the E_η value of CG are in agreement with the values obtained for similar compositions,[22] while the higher T_g range and E_η value of WG may be related to the higher Al_2O_3 and lower Na_2O contents in the composition.

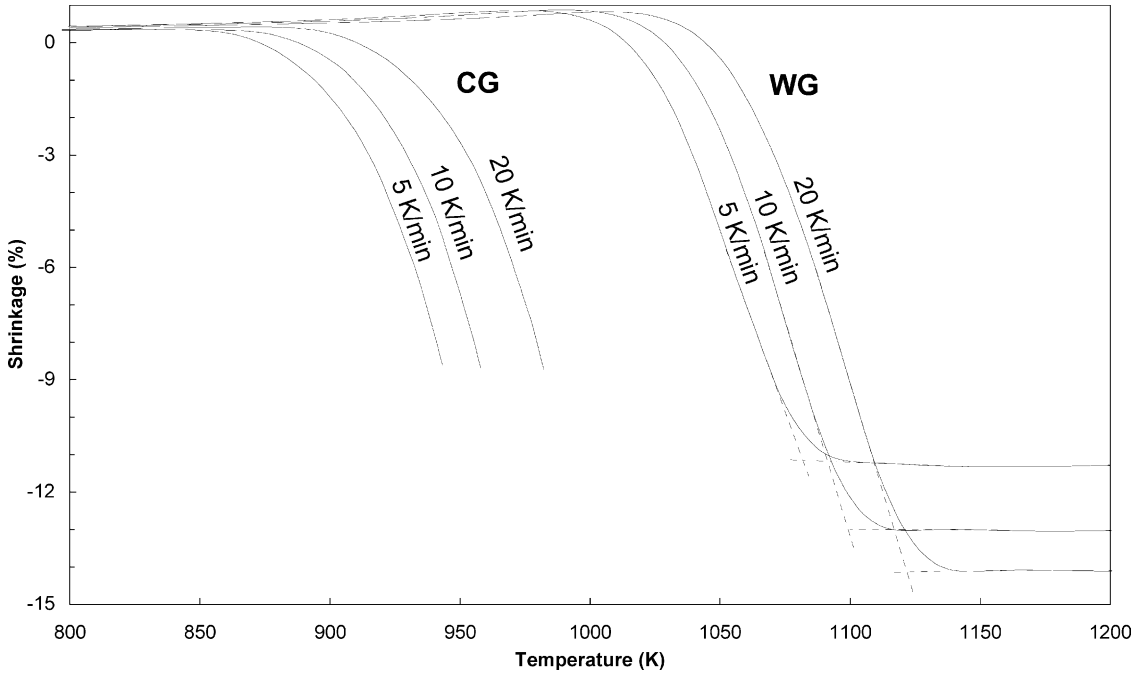

Fig. 1. Dilatometric sintering curves of CG and WG at different heating rates.

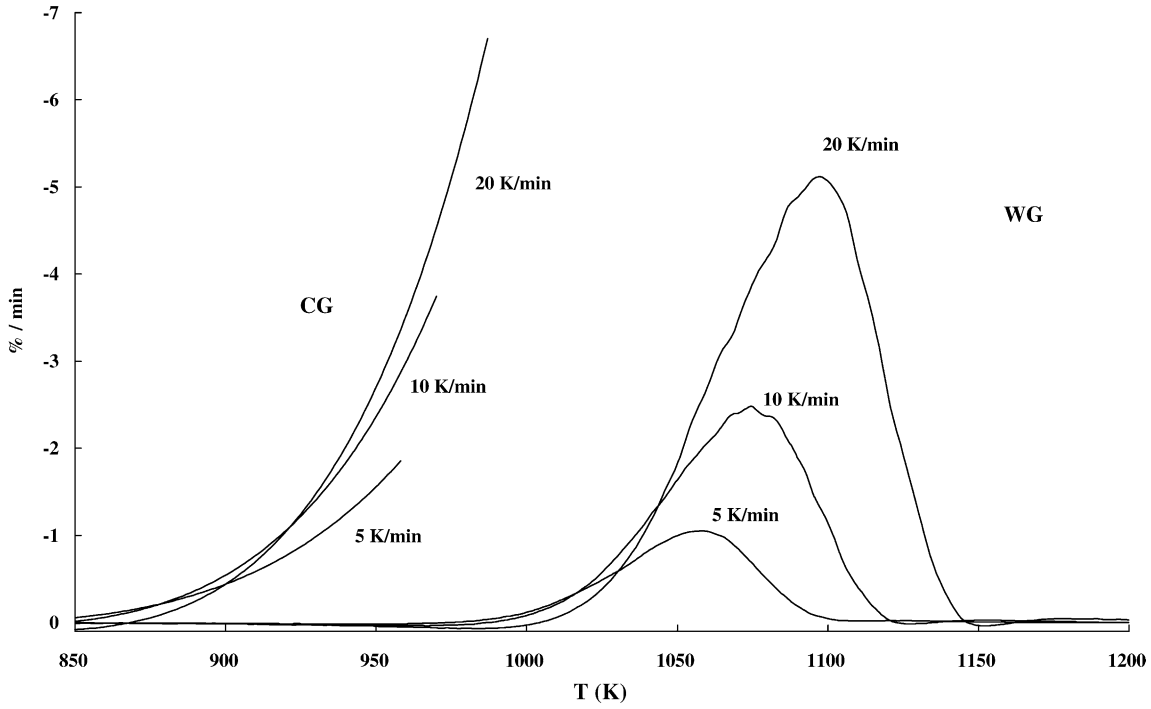

Fig. 2. Sintering rate of WG and CG at different heating rates.

The measured sintering activation energies of CG and WG are lower than the corresponding activation energies of viscous flow due to the external force applied by dilatometer push-rod on the samples[30,31] and the higher sintering temperature range respect to the glass-transition. However, the ratio E_η/E_{sin} for CG is about 2, while for WG it is about 1.5 (for the 1–5% shrinkage range). This difference indicates that the sintering in WG is impeded even at the initial stage of sintering.

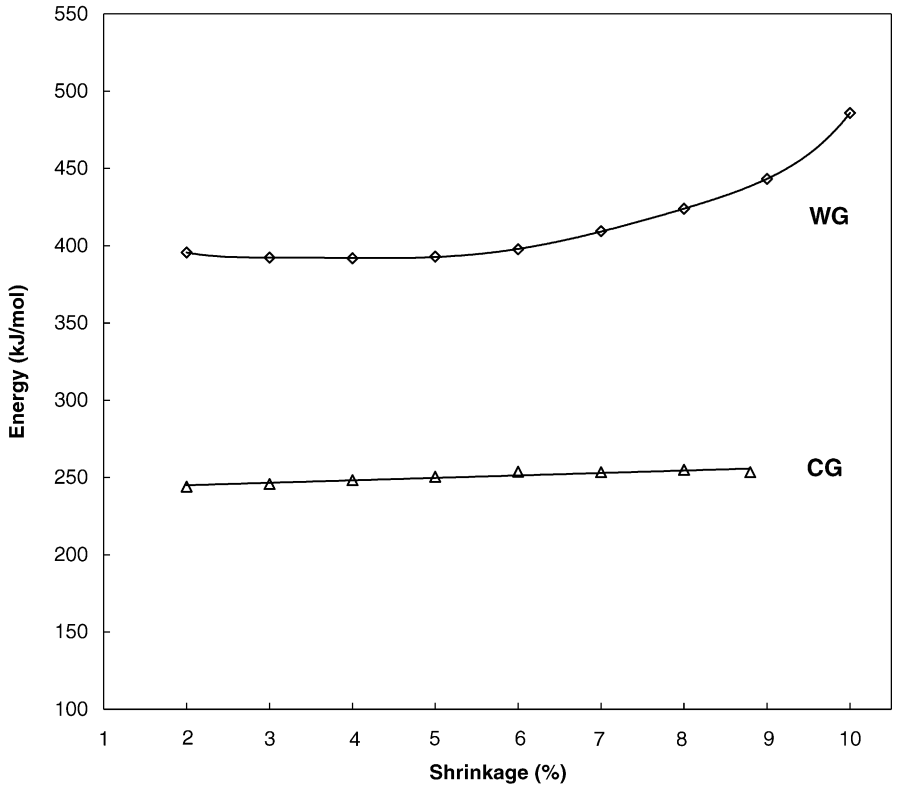

Fig. 3. Sintering activation energy, E_{sin}, of CG and WG as function of the shrinkage.

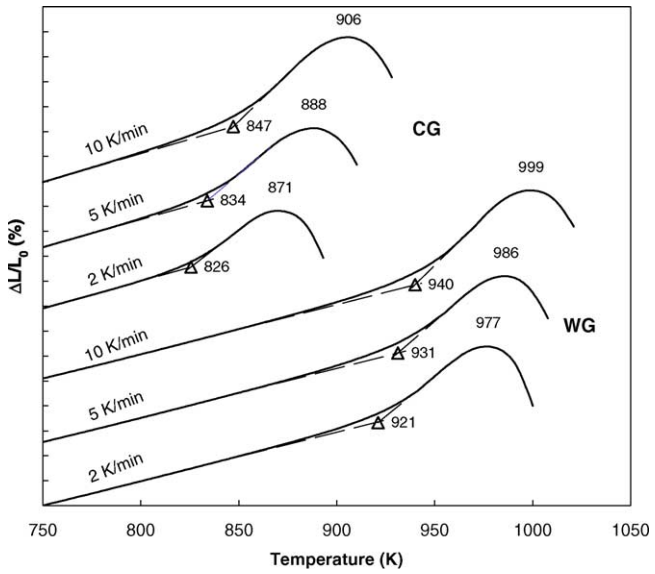

Fig. 4. Dilatometic curves of CG and WG at different heating rates.

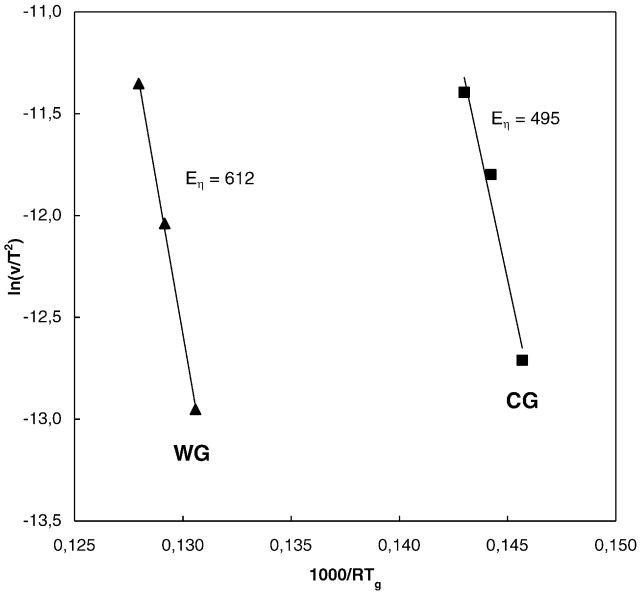

Fig. 5. Plots of $\ln(v/T_g^2)$ vs. $1/T_g$ with corresponding E_η values of CG and WG.

This assumption is confirmed by the fact that the sintering of WG starts at lower shear viscosity than CG. This is highlighted by Fig. 6, where the initial parts of WG and CG sintering curves at 5 K/min (fine lines) are plotted together with the corresponding dilatometric curves (bold lines). In CG glass, the sintering starts immediately after T_g, while in WG the densification occurs at temperatures, near the dilatometric softening point, T_s. Taking into consideration that T_g corresponds to viscosity of $10^{13.3}$ dPa s and T_s to $10^{11.3}$ dPa s[22,23] it can be concluded that in WG the sintering starts at about 100 times lower shear viscosity than CG.

The formation of the crystal phases in the 10^{10}–10^{13} dPa s viscosity range was studied by SEM after heating the samples at 5 K/min and holding them for 1 h at different temperatures, i.e. 823, 873 and 923 K for CG and 923, 973 and 1023 K for WG.

In CG, at 823 K, a smoothing of the particle edges was observed, at 873 K, a neck formation was seen and at 923 K the modification of open in closed porosity occurred. Fig. 7 shows the CG sample at the last temperature. In all samples,

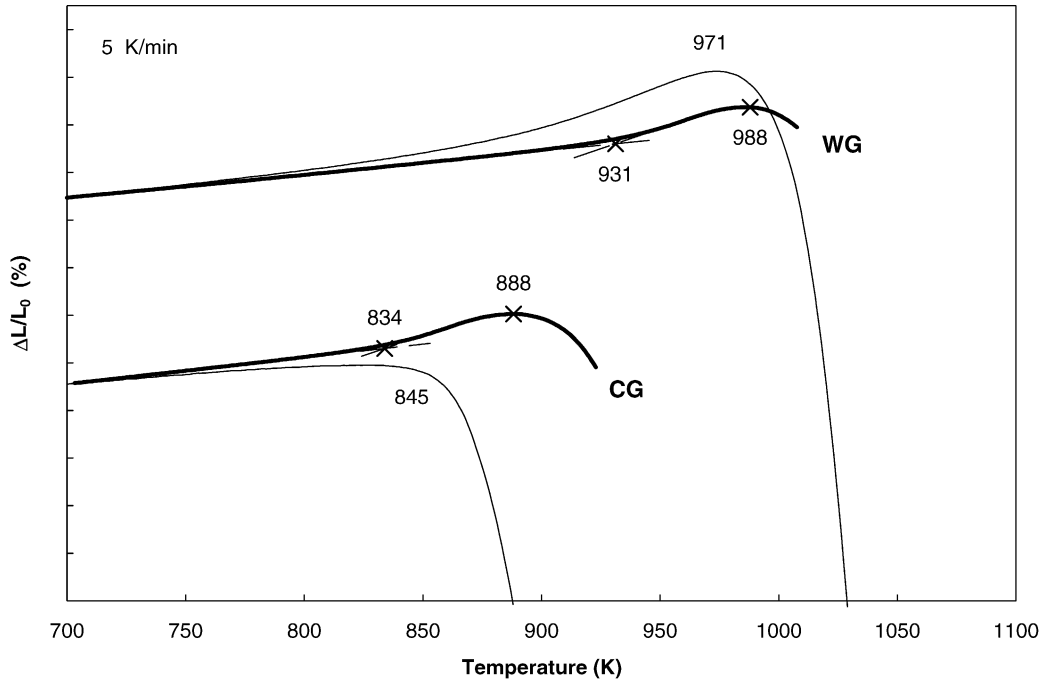

Fig. 6. The initial parts of the WG and CG sintering curves at 5 K/min (fine lines), together with the corresponding dilatometric curves (bold lines).

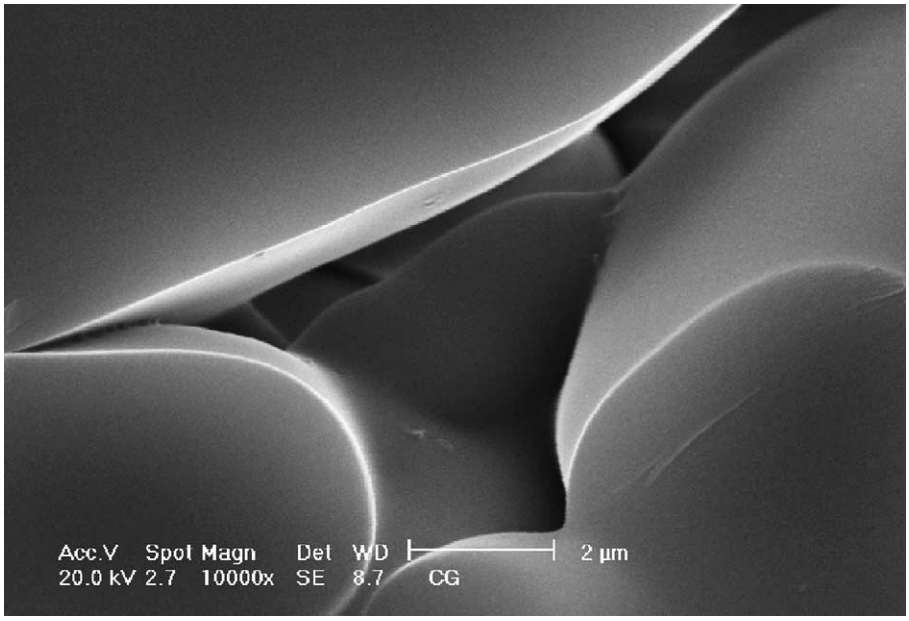

Fig. 7. SEM imagine of fracture of CG sample after 1 h at 923 K (bar: 2 μm).

the grain surface was smooth and free of crystalline formation.

WG sample, treated at 923 K (i.e. in the T_g range) shows a smooth surface without traces of phase formation (Fig. 8), which indicates that the initial delay of the densification process cannot be associated with the surface crystallization process; probably it is a result of the higher apparent viscosity. After 1 h at 973 K, very fine crystals with a size below 0.1 μm were evident on the grain surface (Fig. 9), while after 1 h at 1023 K, the surface crystallization leads to formation of "orange skin" type surface (Fig. 10).

WG sample, heat-treated at 1023 K was crushed and milled to very fine powders (<10 μm) and observed by 200 keV TEM, at 150,000× magnification: the sample highlighted totally amorphous particles together with others showing crystalline formations on one side. It was concluded that the first-ones belonged to the bulk of the sintered particles, while the latter were taken from the surface. Fig. 11 shows the TEM image of one of these particles in which crystals are evident on one side (i.e. the surface of the sample before crushing) and amorphous glass on the other side (i.e. the bulk of the sample). The relative electron diffraction

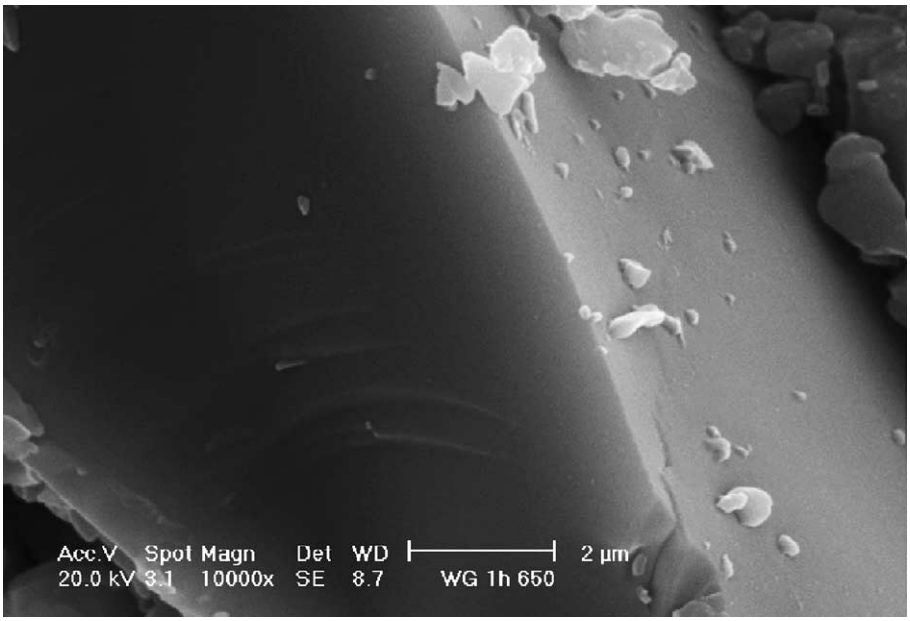

Fig. 8. SEM imagine of fracture of WG sample after 1 h at 923 K (bar: 2 μm).

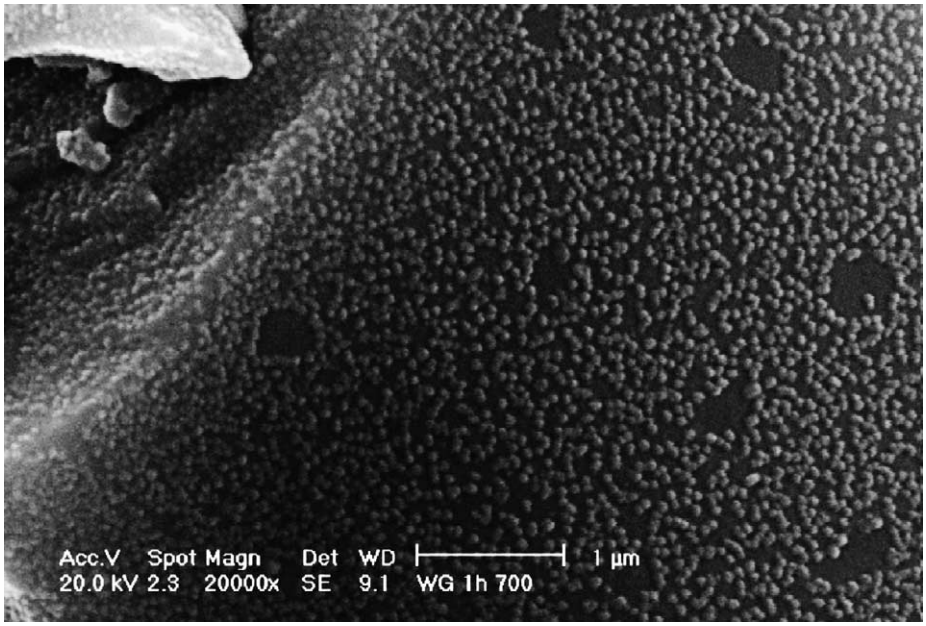

Fig. 9. SEM imagine of fracture of WG sample after 1 h at 973 K (bar: 1 μm).

patterns are shown for comparison. This result shows that the crystallization process at this temperature is only surface induced.

The influence of the phase formation on the densification is shown in Fig. 12, where the WG dilatometric sintering curve at 10 K/min is plotted together with the corresponding DTA trace. The temperature of the first crystallization DTA onset, at 1093 K, is near the sintering onset at 1101 K, which demonstrates that the densification is inhibited by the formation of crystals on the surface of the particles. In the temperature range 1100–1300 K, where the crystallization process occurs, no shrinkage variation was detected by the sensitivity of the employed instrument.

In order to evaluate the amounts of crystalline phase, inhibiting the sintering, samples were heat-treated in an electric furnace, at 5 and 20 K/min, up to the corresponding sintering onset temperatures (1082 and 1122 K, respectively), hold 1 min and quenched in water. The relative XRD spectra are shown in Fig. 13 together with the spectra of the parent glass and the glass-ceramic (1 h at 1173 K). The spectrum of the sample at 5 K/min indicates only initial traces of pyroxene formation (5 ± 3 wt.%), while at 20 K/min the percentage of

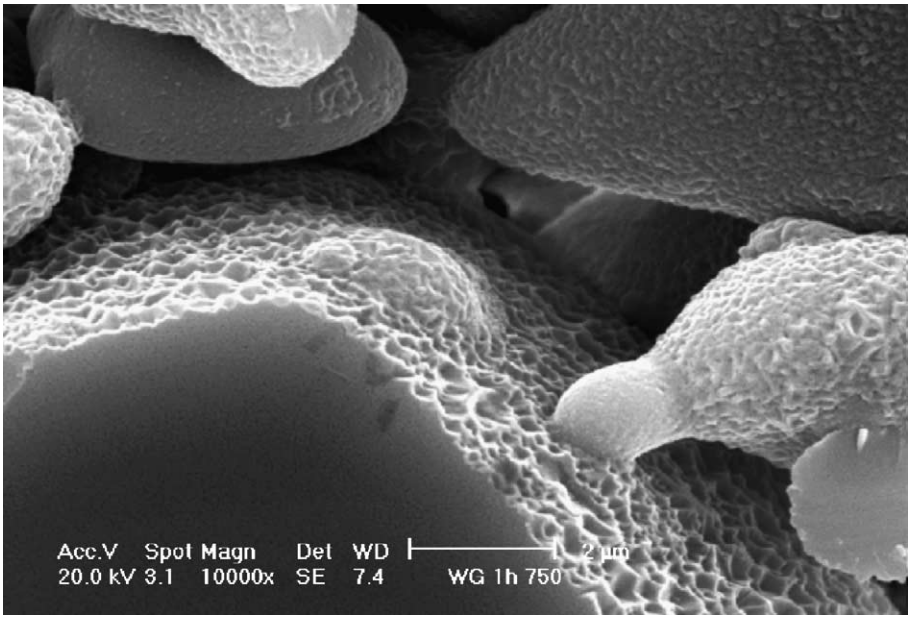

Fig. 10. SEM imagine of fracture of WG sample after 1 h at 1023 K (bar: 2 μm).

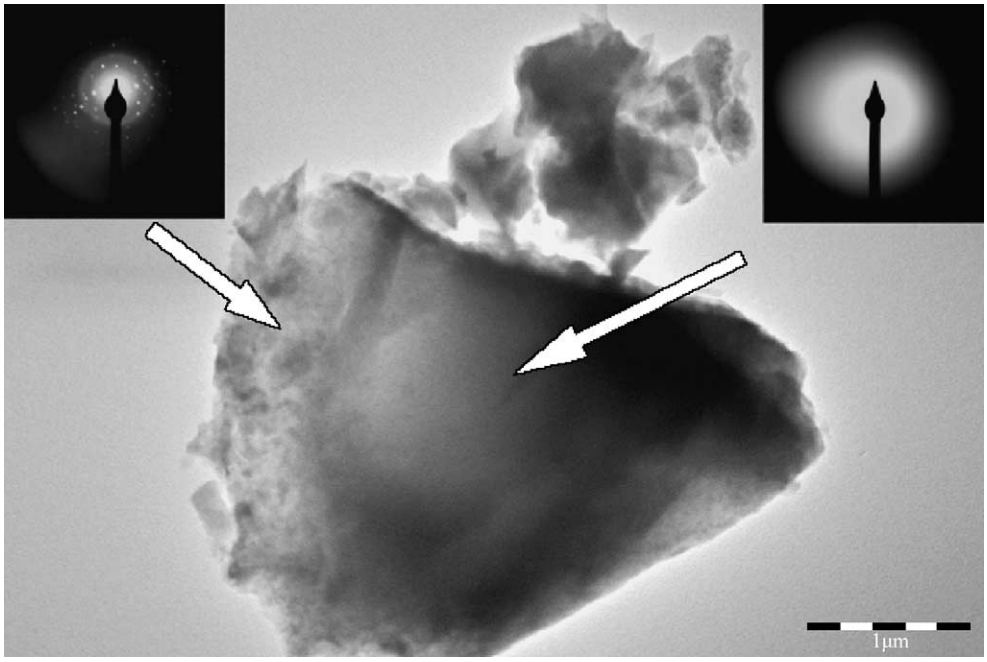

Fig. 11. TEM image of a WG fine particle with polycrystalline (left side) and amorphous (right side) parts, together with the relative electron diffraction patterns (bar: 1 μm).

crystal phase was estimated as 13 ± 3%; in the glass-ceramic a 67 ± 3 wt.% crystal phase, constituted by pyroxene, anorthite and gehlenite, was evaluated.

At 20 K/min the densification stops after the formation of a higher amount of crystal phase, because the formation of the crystals takes place at lower viscosity. As a result, a higher percentage of crystallization can be attained before that the densification is inhibited by the increase of the apparent viscosity. Therefore, as previously reported in other studies,[10,14,15,20,32] sintering is improved by faster heating rates.

Moreover, sintering at high heating rates positively influences the mechanical properties, because higher densification degree, i.e. lower porosity is attained in the samples (see Fig. 1). The evaluation of the bending strength and the Young modulus of the glass-ceramic heated at 20 K/min showed

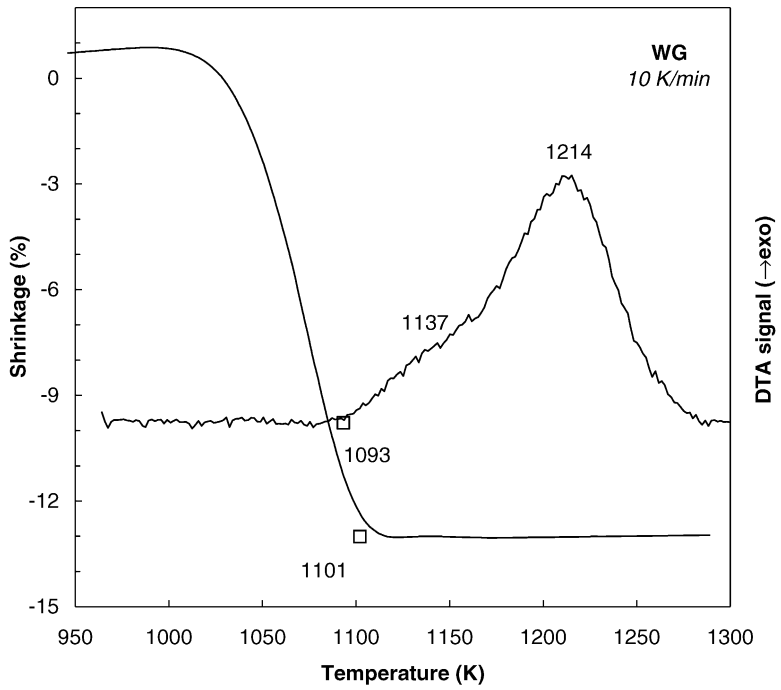

Fig. 12. Dilatometric sintering curve and DTA trace of WG at 10 K/min.

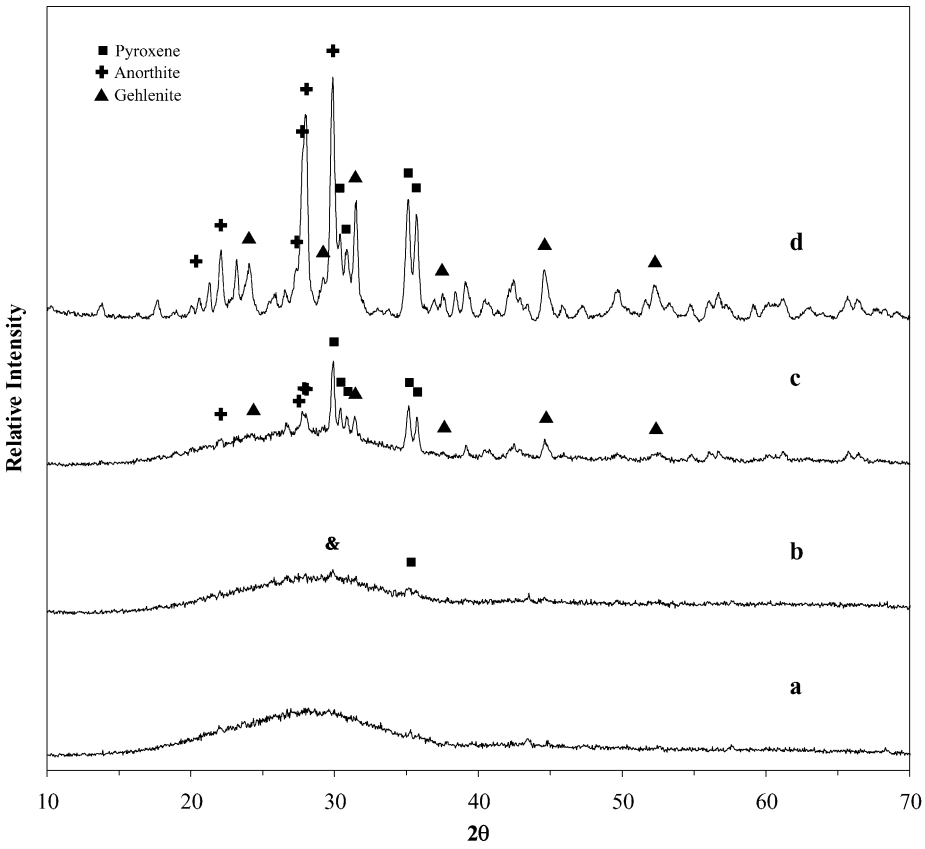

Fig. 13. XRD spectra: parent glass (a); sample, heat-treated at 5 K/min up to 1082 K (b); sample, heat-treated at 20 K/min up to 1173 (c); final glass-ceramics (d).

values of 59 ± 5 MPa and 45 ± 4 GPa while for the samples heated at 5 K/min the obtained values are 49 ± 4 MPa and 42 ± 5 GPa, respectively.

5. Conclusions

As shown by the sintering WG curve, plotted together with the DTA trace, the densification process resulted to be influenced by the crystalline formations, i.e. the sintering is interrupted by the beginning of the pyroxene crystal phase formation.

The high value of E_{sin} of WG and the increasing trend after 5% shrinkage supported the sinter-crystallization behaviour of the MSWI investigated glass.

Since the crystallization and the sintering processes occurred simultaneously, the densification was inhibited and a residual porosity remained in the glass-ceramic. Improved sintering was obtained by applying high heating rate, which also had a positive effect on the mechanical properties of the glass-ceramic material.

References

1. Frenkel, J., Viscous flow of crystalline bodies under the action of surface tension. *J. Phys. USSR 9*, 1945, **5**, 385–391.
2. Kingery, W. D., *Introduction to Ceramics*. John Wiley & Sons, New York, 1974.
3. Geguzin, Y. E., *The Physics of Sintering*. Nauka, Moscow, 1984 (in Russian).
4. Olevsky, E., Theory of sintering: from discrete to continuum. *Mater. Sci. Eng.*, 1998, **R23**, 41–100.
5. Höland, W. and Beall, G., *Glass-Ceramics Technology*. The American Ceramics Society, Westerville, 2002.
6. Müller, R., Kirsh, M. and Lorenz, H., Surface crystallization—a limiting effect of sintering glass powders. In *Proceedings of the 15th Congress on Glass*, 1989, pp. 334–338.
7. Müller, R., On the kinetics of sintering and crystallization of glass powders. Proceedings of 5th Otto Shott Coll., Jena, 1994, pp. 93–99. *Glastech. Ber. Glass. Sci. Technol.*, 1994, **67C**.
8. Zanotto, E. and Prado, M., Isothermal sintering with concurrent crystallisation of monodispersed and polydispersed glass particles. Part 1. *Phys. Chem. Glasses*, 2001, **42**(3), 191–198.
9. Rabinovich, E. M., Review: preparation of glass by sintering. *J. Mater. Sci.*, 1985, **20**, 4259–4297.
10. Karamanov, A., Penkov, I. and Gutzow, I., A new marble-like glass-ceramic material. In *Proceedings of Fundamentals of Glass Science and Technology—ESG*, 1993, pp. 675–679.
11. Gutzow, I., Paskova, R., Karamanov, A. and Schmelzer, J., The kinetics of surface induced sinter-crystallization and the formation of glass-ceramic materials. *J. Mater. Sci.*, 1998, **33**(21), 5265–5273.
12. Boccaccini, A., Bucker, M. and Bossert, J., Glass and glass-ceramics from coal fly-ash and waste glass. *Tile Brick Int.*, 1996, **12**(6), 515–518.
13. Winter, W., Sintering and crystallization of volume- and surface-modified cordierite glass powders. *J. Mater. Sci.*, 1997, **32**, 1649–1655.

14. Sujirote, K., Rawlings, R. D. and Rogers, P. S., Effect of fluoride on sinterability of a silicate glass powder. *J. Eur. Ceram. Soc.*, 1998, **18**, 1325–1330.
15. Boccaccini, A. R., Stumpfe, W., Taplin, D. M. R. and Ponton, C. B., Densification and crystallization of glass powder compacts during constant heating rate sintering. *Mater. Sci. Eng.*, 1996, **A219**, 26–31.
16. Strnad, Z., *Glass-Ceramic Materials*. Elsevier, Amsterdam, 1986.
17. Boccacini, A., Schawohl, G., Kern, H., Schunck, B., Rincon, J. and Romero, M., Sintered glass-ceramics from municipal incinerator fly ash. *Glass Technol.*, 2000, **41**, 99–105.
18. Ferrarsi, M., Salvo, M., Smeacetto, F., Augier, L., Barbieri, L., Corradi, A. *et al.*, Glass matrix composites from solid waste materials. *J. Eur. Ceram. Soc.*, 2001, **21**, 453–460.
19. Cheng, T. W., Ueng, T. H., Chen, Y. S. and Chiu, J. P., Production of glass-ceramic from incinerator fly ash. *Ceram. Int.*, 2002, **28**, 779–783.
20. Karamanov, A., Pelino, M. and Hreglich, A., Sintered glass-ceramics from MSW-incinerator fly ashes part I: the influence of the heating rate on the sinter-crystallisation. *J. Eur. Ceram. Soc.*, 2003, **23**, 827–832.
21. Perez-Maqueda, L. A., Criado, J. M. and Real, C., Kinetics of the initial stage of sintering from shrinkage data: simulation determination of activation energy and kinetic model from a single nonisothermal experiment. *J. Am. Ceram. Soc.*, 2002, **85**(4), 763–768.
22. Scholze, H., *Glass Nature, Structure and Properties*. Springer-Verlag, Berlin, 1990.
23. Feltz, A., *Amorphe und Glasartige Anorganische Festkorpen*. Academie-Verlag, Berlin, 1983.
24. Sestak, J., *Thermophysical Properties of Solids—Their Measurements and Theoretical Thermal Analysis*. Academia, Prague, 1984.
25. Chen, H., A method for evaluating viscosities of metallic glasses from the rates of thermal transformations. *J. Non-Cryst. Solids*, 1978, **27**, 257–263.
26. Ray, C. S. and Day, D. E., Nucleation and crystallization in glasses as determined by DTA. Ceramic transactions. Nucleation and crystallization in liquids and glasses. *Am. Ceram. Soc.*, 1992, **30**, 207–224.
27. Kissinger, H., Reaction kinetics in differential thermal analysis. *Anal. Chem.*, 1957, **29**, 1702–1706.
28. Thakur, R., Determining the suitability of nucleation agents for glass ceramics. In *Advanced in Nucleation and Crystallization of Glasses. American Ceramics Society Glass Division Symposia*, 1971, pp. 166–172.
29. Ozawa, T., Kinetics of non-isothermal crystallization. *Polymer*, 1971, **12**, 150–158.
30. Paganelli, M., Using the optical dilatometer to determine sintering behaviour. *Am. Ceram. Soc. Bull.*, 2002, **81**(11), 25–30.
31. Speyer, S. F., *Thermal Analysis of Materials*. Marcel Dekker, Inc., New York, 1994.
32. Panda, P. and Ray, R., Sintering and crystallization of glass at constant heating rate. *J. Am. Ceram. Soc.*, 1989, **72**(8), 1564–1566.